International Journal of Engineering &Technology, 7 (4) (2018) 6747-6755

SPC

International Journal of Engineering & Technology

Website: www.sciencepubco.com/index.php/IJET
doi: 10.14419/ijet.v7i4.20322
Research paper



Triangular modeling using Delaunay based region growing approach

Vandana Agrawal *

Department of Mechanical EngineeringMotilal Nehru National Institute of Technology Allahabad, Prayagraj-211004, India
**Corresponding author E-mail:vandana@mnnit.ac.in*

Abstract

In the present work a Delaunay based region growing algorithm is proposed to create triangulated model from the unorganized data set obtained by coordinate measuring machine (CMM).The algorithm maintains the advantages of both Delaunay based and region growing approaches. In this algorithm a data structure is created which contains the information about the edges and the vertices of all the triangles created by Delaunay triangulation. Further a region growing process is used by initiating a seed triangle. The new triangles selected from Delaunay data structure are incrementally added to the region. One of the advantage of suggested algorithm is that no post processing is required as hole filling and topological examination is done during the growing process itself. The region growing takes place more smoothly along the faces of the object when algorithm is applied by incorporating hole filling process and topological examination. Further, the holes and topological disorders like neck vertices and non-manifold surface disappeared when algorithm is applied by incorporating hole filling process and topological examination in comparison to the modelling excluding them. The triangulated model created so can be used for subsequent processes of reverse engineering like segmentation and surface fitting.

Keywords:*Triangulation; Reverse Engineering; Region growing.*

1. Introduction

The data of physical objects are generally recorded by different kind of scanners like Coordinate Measuring Machine (CMM), Optical Scanner and magnetic resonance etc. For an object with arbitrary shape, these data points are in the form of unorganized point cloud. However, point cloud representation of the object is ambiguous, as the object geometry is only known at the finite number of discrete locations, while the object topology is totally unknown. The object topology can be recovered if the model is represented by continuous manifold surface. One of such representation is in the form of triangular mesh. The object surface represented by triangular mesh is not only visually pleasant, but also facilitates many subsequent processes of reverse engineering like segmentation [1], [2] and surface fitting [3], [4].

In literature [5]-[13] several algorithms have been proposed to create the triangulated models. They can broadly be classified into two main categories:

1) Delaunay based approach [6], [7].
2) Region growing approach [5], [8]-[13].

In Delaunay based approach a geometrical structure is created from the scanned data using either Delaunay triangulation [14] or Voronoi diagram [6]. If the scanned data is in the form of 3D points then the geometrical structure created consists of various tetrahedrons joining them. Further, to create triangulated model certain faces of these tetrahedrons are extracted. In literature many algorithms [6], [7] have been suggested to extract these faces, such that they represent the surface of the model. Though these algorithms are systematic and robust, however, they are computationally more expensive.

The region growing approach begins by initiating an appropriate triangle named as seed triangle [5], [8]-[13] on the surface of the model. The region growing approach is faster comparative to Delaunay based approach, however the reconstruction quality heavily depends on the user defined parameters e.g. maximum point to point distance [15], which depends on the sampling density and cannot be assigned easily[5], [8]-[13]. Another drawback of region growing process is that it leaves behind holes [5], [8]-[13]. Hence, an appropriate hole-filling procedure is always required.

In the present work a Delaunay based region growing algorithm is proposed to create triangulated model from the unorganized data set obtained by high precision 3D coordinate measuring machine (CMM) shown in Fig.1. The specifications of machine are given in Table1. In this algorithm first a data structure is created which contains the information about the edges and the vertices of all the triangles created by Delaunay triangulation. Further a region growing process is used by initiating a seed triangle. The new triangles attached to the region are selected from the data structure mentioned above. One of the important features of the algorithm proposed is that hole-filling and topological examination for non-manifolds and neck vertices that take place during the region growing process itself. Hence no post processing of the model is required. The algorithm has been applied on the unorganized data collected for a telephone receiver (Fig.2(a)). The results are found to be satisfactory with significantly less number of holes in comparison to earlier approaches. Further, topological disorders were also not present in the final model.

Copyright ©2018 Vandana Agrawal. This is an open access article distributed under the Creative Commons Attribution License, which permits unrestricted use, distribution, and reproduction in any medium, provided the original work is properly cited.

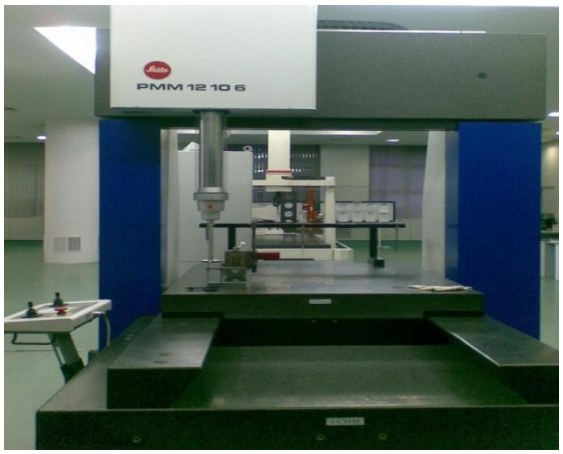
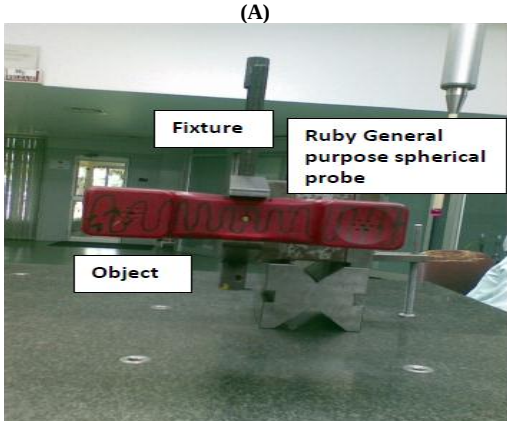


Fig. 1: 3D Coordinate Measuring Machine.

Table 1: The Specifications of CMM

1.	Make	LEITZ, Germany
2.	Model	PMM 12 10 6
3.	Manufacturer	BROWN & SHARPE, ASIA PACIFIC OFFICE
4.	Measuring range	X=1200mm, Y=1000mm, Z=600mm
5.	Linear U1(µm) (L in mm)	0.5+L/700µm
6.	Volumetric U2(µm)(L in mm)	0.8+L/450µm
7.	Gauge Accuracy In volume 600X600X300mm	0.3+L/1000µm
8.	Minimum resolution	0.1µm
9.	Probing Speed	0.1-3 mm/sec
10.	Max. Scanning Speed	50 mm/s
11.	Max. Probe pin wt.	650 gm (without Probe holder)
12.	Pick up of measuring points	200 points/sec
13	Operating Temperature	$20^0 \pm 0.5^0$C

(A)



(B)

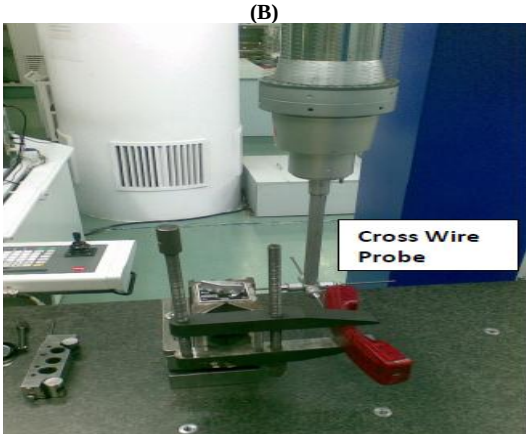


Fig. 2: Object Fitted on CMM Along with (A) Ruby General Purpose Spherical Probe (B) Cross Wire Probe.

2. Data acquisition

The telephone receiver was placed on the granite table of CMM with the help of a fixture as shown in Fig.2(a). Scanning has been done with the help of ruby general purpose spherical probe (Fig.2(a)), for five faces of the object, however for sixth face lying underneath the object it is done using cross wire probe (Fig.2(b)). The head of CMM was positioned and translated by the joystick control of the machine. The data points for the portion of telephone receiver where the fixture was mounted could not be captured. Coordinates were recorded by setting the origin at the centre of the reference ball mounted on CMM. The data set obtained so, has been stored into a data file. Further, the origin has been shifted to the first point measured and then all the data were translated accordingly. The resulting cloud data of the object are shown in Fig. 3. It can be seen in Fig.3 that point cloud is missing from the place where fixture has been mounted.

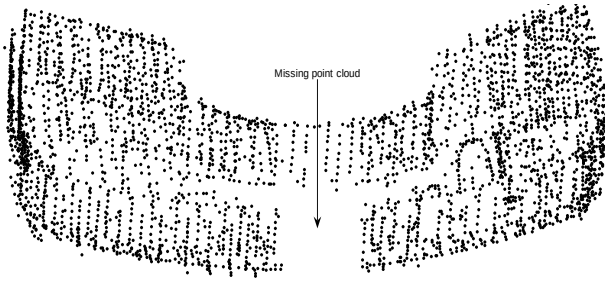


Fig. 3: Cloud Data Obtained after Measurement with CMM.

3. Data structure

A set of x, y and z coordinates is obtained after measurement of various points of object by coordinate measuring machine. In present work cloud data containing 3299 points shown in Fig.3 are obtained. These data points are further connected by Delaunay triangulation and as a result a set of tetrahedrons is formed. In this process no point is left unconnected. Due to this no point will be present inside the circum-sphere of any individual tetrahedron. Delaunay triangulation can be explained by taking a simple case of 2-dimensional Euclidean space with the help of fig. 4[16]. Here points a, b, c, d, e, f, g, h, i and j are in a plane and by Delaunay triangulation triangles like abc, bcd, cde etc. are formed. Through each triangle circum-circle is drawn and it can be seen that no circum-circle is containing any unconnected point. In MATLAB, T=delaunay3(x,y,z) returns an array T, each row of which contains the indices of the points in (x,y,z) that make up a tetrahedron in the tessellation of (x,y,z). For example Table-2 represents the coordinates of n points.

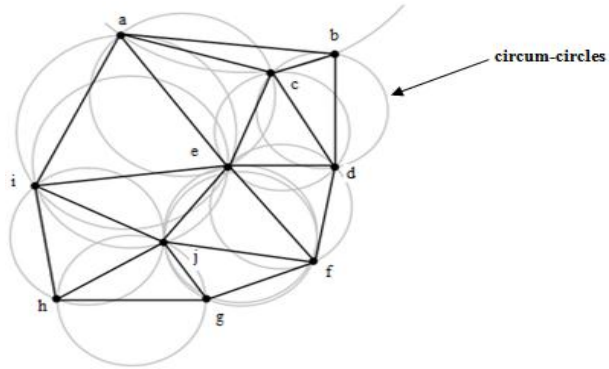


Fig. 4: Delaunay Triangulation of Points in Plane with Their Circum-Circle.

Table 2: Coordinates of N Points

v_1	x_1	y_1	z_1
v_2	x_2	y_2	z_2
v_3	x_3	y_3	z_3

----	----	----	----
----	----	----	----
----	----	----	----
----	----	----	----
v_n	x_n	y_n	z_n

After applying delaunay3 function in MATLAB tetrahedrons are formed by connecting these points. These tetrahedrons are represented by the indices of the points as shown in Table-3. So, the function delaunay3 is applied on cloud data points of Fig.3. As a result a set of 20,019 tetrahedrons were obtained. Fig.5 (a) shows tetrahedrons formed on vertices v_1-v_7. Also, one of the tetrahedrons defined by its four vertices (v_1, v_2,v_3, v_4) is shown in Fig.5 (b). It can be seen from Fig.5(b) that the tetrahedron is having four triangular faces viz. (v_1,v_2 ,v_3), (v_2 ,v_3 ,v_4), (v_3 ,v_4 ,v_1) and (v_4 ,v_1 ,v_2). Since some of the triangles are common with other tetrahedrons and in view of this a total of 40,283 triangles are extracted from Delaunay triangulation for total 20,019 tetrahedrons. Let us denote the set of these triangles as DT=[t_1 ,t_2 ,t_3 ,……,$t_{40,283}$]. During the region growing process the triangles are extracted from this set DT and in each iteration the number of triangles go on decreasing and DT gets modified as per procedure explained in section 4. It is obvious from the above description that these triangles will be shown by their vertices like v_1, v_2, v_3. These vertices are represented by their coordinates. Further the edges of the triangles are represented like v_1v_2; v_2v_3 and v_3v_1 and these edges are denoted by e_1, e_2 and e_3 as shown in Fig.6. Hierarchy of the data structure used in the work is represented in Fig. 7.

Table 3: Tetrahedrons Formed from N Points of Table-2

1	v_1	v_2	v_3	v_7
2	v_1	v_7	v_3	v_4
3	v_7	v_3	v_6	v_5
4	v_1	v_7	v_3	v_5
----	----	----	----	----
----	----	----	----	----
----	----	----	----	----
----	----	----	----	----

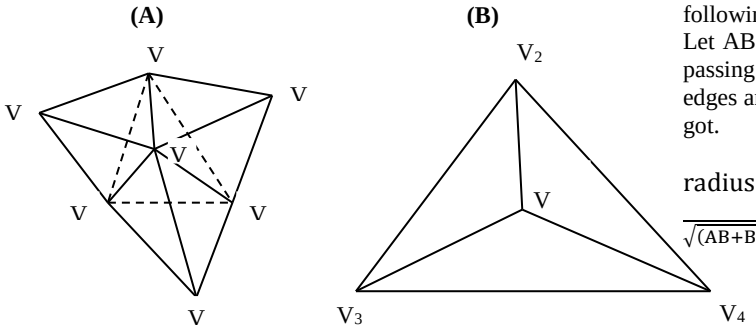


Fig. 5: A) Tetrahedrons Formed on Vertices V_1-V_7, B): A Tetrahedron Made with Vertices V_1, V_2, V_3, V_4.

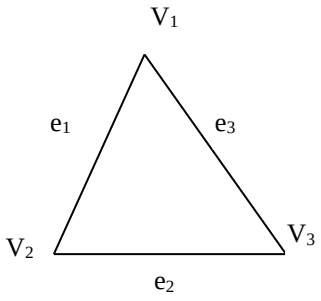


Fig. 6:A Triangle Shown by Its Vertices and Edges

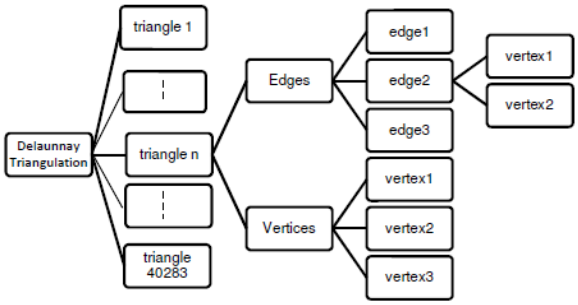


Fig. 7: Hierarchy of Data Structure.

4. Region growing algorithm

As explained earlier the triangles extracted should lie on the surface of the object and not at the interior. However some of the triangles are formed at the interior of the object. But finally a water tight triangulated manifold model is required which requires triangular facets only on the surface of the object. In view of this triangles formed at interior should be eliminated. So the triangles are selected from the set DT obtained from Delaunay triangulation. For this purpose region growing algorithm is used. This algorithm initially requires a seed triangle and then the growth of the region of the surface of the object takes place around the seed triangle.

4.1. Initial triangle selection used as seed triangle

To start the region growing process an initial triangle is selected from the set of 40,283 triangles extracted from data structure described earlier. For this, first a vertex v_i having maximum value of z coordinate [17] out of 3299 cloud data points is obtained. Further, set of triangles incident on vertex v_i is extracted from the data structure. The circum-radii of triangles were determined using the following procedure.

Let ABC is a triangle (Fig.8), O is the centre of the circum-circle passing through the vertices A,B and C. Further the lenghts of edges are taken as AB, BC and CA. Using Heron's formula eq.(1) is got.

$$\text{radius of circum circle} = \frac{AB \times BC \times CA}{\sqrt{(AB+BC+CA)\times(-AB+BC+CA)\times(AB-BC+CA)\times(AB+BC-CA)}} \quad (1)$$

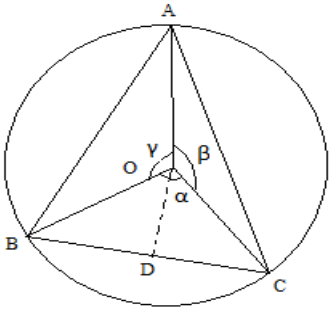


Fig. 8:A Triangle ABC with Its Circum-Circle Having Centre O.

Now, taking the coordinates of vertices A, B & C as given below
Coordinates of A(x_a , y_a , z_a)
Coordinates of B(x_b , y_b , z_b)
Coordinates of C(x_c , y_c , z_c)
Using the co-ordinates the lengths of edges AB, BC and AC are given by eqs.(2), (3) & (4).

$$AB = \sqrt{(x_a - x_b)^2 + (y_a - y_b)^2 + (z_a - z_b)^2} \quad (2)$$

$$BC = \sqrt{(x_b - x_c)^2 + (y_b - y_c)^2 + (z_b - z_c)^2} \quad (3)$$

$$CA = \sqrt{(x_c - x_a)^2 + (y_c - y_a)^2 + (z_c - z_a)^2} \quad (4)$$

Further taking OA = OB = OC = radius of circle = r and α, β and γ as the angle subtended by edges BC, CA and AB on the centre. Now a perpendicular OD is dropped from the centre O on the edge BC. Since OB and OC are equal and therefore BD is equal to DC and angle BOD=α/2. The angle α is given by eq.(5)

$$\sin(\alpha/2) = \frac{BC}{2\times r} \quad (5)$$

Now, substituting the value of BC from eq.(3) , eq.(6) is obtained or

$$\sin(\alpha/2) = \frac{\left(\sqrt{(x_b-x_c)^2+(y_b-y_c)^2+(z_b-z_c)^2}\right)/2}{r} \quad (6)$$

Similarly the angles β and γ can be expressed by eqs.(7) and (8) respectively as

$$\sin(\beta/2) = \frac{\left(\sqrt{(x_c-x_a)^2+(y_c-y_a)^2+(z_c-z_a)^2}\right)/2}{r} \quad (7)$$

$$\sin(\gamma/2) = \frac{\left(\sqrt{(x_a-x_b)^2+(y_a-y_b)^2+(z_a-z_b)^2}\right)/2}{r} \quad (8)$$

After determining the circum-radii the triangles were arranged in order of their increasing values of circum-radii starting from min-imum circum-radius triangle. Further angles α, β and γ computed from eqs.(6), (7) and (8) can be used to detect the skewed triangles to avoid them. Now the angles between the normal to triangle and positive z direction are computed following the procedure given below.

Fig.9 shows the directions of x, y and z axes and Figs.10 & 11 shows the triangles with vertices v_1, v_2& v_3. Further, any triangular face will have two directions of normal. One, which is computed considering orientation of edge vectors to be in clockwise direction and other to be in counter-clockwise direction. It can be seen from Fig.10 that if the triangle lies in x-y plane, then by applying right hand rule, the normal comes out to be in the direction of positive z-axis. Therefore, for any triangle counter-clockwise orientation of the edge vectors are considered. If (x_1, y1, z1), (x_2, y2, z2) and (x_3, y3, z3) are the coordinates of the tri-angle vertices v_1, v_2 and v_3 respectively then the edge vectors in counter-clockwise direction are given by eqs. (9) & (10)

$$E_1 = v_1 - v_2 = (x_1 - x_2)\hat{\imath} + (y_1 - y_2)\hat{\jmath} + (z_1 - z_2)\hat{k} \quad (9)$$

$$E_2 = v_2 - v_3 = (x_2 - x_3)\hat{\imath} + (y_2 - y_3)\hat{\jmath} + (z_2 - z_3)\hat{k} \quad (10)$$

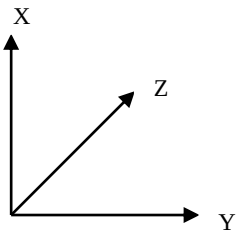


Fig. 9: Direction of X, Y and Z Axes.

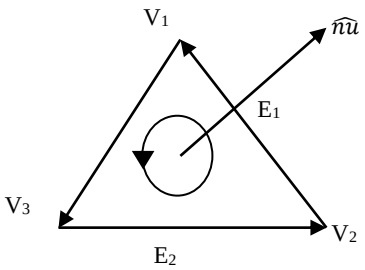


Fig. 10: The Direction of the Unit Normal $\widehat{nu}$.

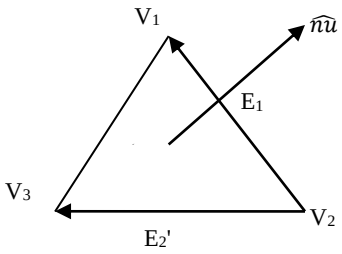


Fig. 11: Edge V_2V_3 Represented by Vector E_2'.

When the orientation of the vertices is counter-clockwise the unit normal vector can be given as

$$\widehat{nu} = \frac{E_2XE_1}{|E_2XE_1|} \quad (11)$$

Further if edge v_2v_3 is represented by vector E_2' as shown in fig.11 then unit normal vector $\widehat{nu}$ can also be represented by eq.(12) as follows

$$\widehat{nu} = \frac{E_1XE_2'}{|E_1XE_2'|} \quad (12)$$

Where,

$$E_2' = v_3 - v_2 = (x_3 - x_2)\hat{\imath} + (y_3 - y_2)\hat{\jmath} + (z_3 - z_2)\hat{k} \quad (13)$$

Now the angle θ_z between the unit normal of the triangle and z-axis is given by the following eq.(14)

$$\theta_z = \cos^{-1}(\widehat{nu}.\hat{k}) \quad (14)$$

The first triangle for which this angle comes out to be less than π/2 [17] is selected as seed triangle t_i. This triangle is the first triangle of the growing region. Now, if growing region is repre-sented by set S which consists of triangles added to the growing region, then at this stage growing region is represented by S=[t_i]

4.2. Region growing process

All the edges of triangles, in growing region S, which are shared only by one triangle is known as boundary edges and the set of all the boundary edges is represented by E. At this point of time all the edges of seed triangle are boundary edges and set of boundary edges is given by E= [e_1, e2, e3]. Now, the triangles incident (Fig. 12) on each of the edges e_1, e2 and e_3 are extracted from set DT described earlier in section 3. These sets of triangles for edges e_1, e2 and e_3 are given by T_1= [t_{11} t_{12} t_{13} t_{14} t_{15}], T_2= [t_{21} t_{22} t_{23} t_{24}] and T_3= [t_{31} t_{32} t_{33}] respectively.

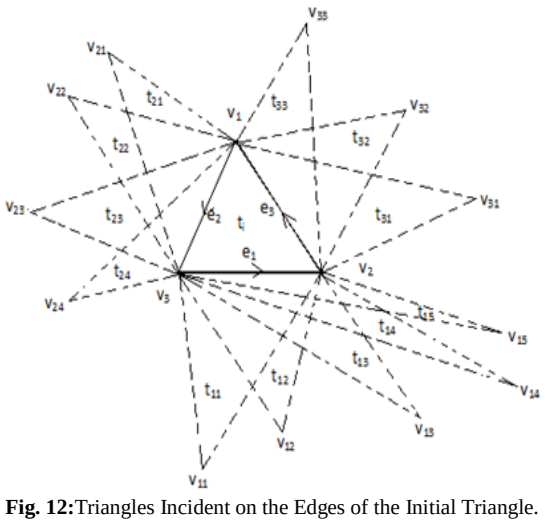


Fig. 12: Triangles Incident on the Edges of the Initial Triangle.

Further the set of boundary triangles corresponding to edges E=[e_1 e_2 e_3] is extracted from the growing region S Let T_b represents the set of boundary triangles then T_b=[t_{b1} t_{b2} t_{b3}]. At this moment growing region has only one triangle t_i , hence t_{b1} =t_{b2} =t_{b3} =t_i. Now, the triangles to be inserted in growing region are computed as follows.

First of all the included angle θ between incident triangles on boundary edge and corresponding boundary triangle is computed as explained below.

Included angle between the two adjacent triangles is same as the angle between their normals. Therefore on a triangle say t_1 in Fig.13 if the orientation of the vertices is taken as counter-clockwise then according to right hand rule described earlier the direction of the unit normal should be nu_1 as shown in the same figure. Also, its value can be found out by first computing the vectors along its two of the edges by eqs.(15) and (16) as follows

$$e_{11} = v_{11} - v_{12} = (x_{11} - x_{12})\hat{i} + (y_{11} - y_{12})\hat{j} + (z_{11} - z_{12})\hat{k} \quad (15)$$

$$e_{12} = v_{13} - v_{12} = (x_{13} - x_{12})\hat{i} + (y_{13} - y_{12})\hat{j} + (z_{13} - z_{12})\hat{k} \quad (16)$$

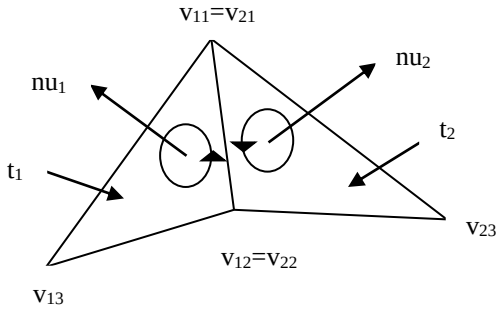


Fig. 13: Direction of Normal on Adjacent Triangles.

Now,using the counter-clockwise orientation of the vertices the unit normal on triangle t_1 is computed using eq.(17).

$$\widehat{nu_1} = \frac{e_{11} X e_{12}}{|e_{11} X e_{12}|} \quad (17)$$

On the adjacent triangle t_2 for computing the unit normal nu_2 the orientation of the vertices should be kept same i.e. in counetr-clockwise direction. Again, for triangle t_2 the vectors along its edges can be computed by eqs. (18) & (19) as follows

$$e_{21} = v_{21} - v_{22} = (x_{21} - x_{22})\hat{i} + (y_{21} - y_{22})\hat{j} + (z_{21} - z_{22})\hat{k} \quad (18)$$

$$e_{22} = v_{23} - v_{22} = (x_{23} - x_{22})\hat{i} + (y_{23} - y_{22})\hat{j} + (z_{23} - z_{22})\hat{k} \quad (19)$$

Unit normal nu_2 on triangle t_2 can be computed by eq.(20)

$$\widehat{nu_2} = \frac{e_{22} X e_{21}}{|e_{22} X e_{21}|} \quad (20)$$

Now, the included angle θ between the triangles t_1 and t_2 is computed using eq.(21).

$$\theta = \cos^{-1}(\widehat{nu_1}.\widehat{nu_2}) \quad (21)$$

Further the circum-radius of each incident triangle is calculated following the procedure given earlier.

As shown in Fig.14 the triangles with minimum circum-radius and θ<5π/6 are added in growing region S [14],[18].

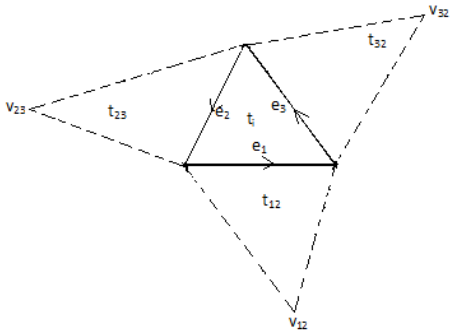


Fig. 14: The New Region Formed on the Initial Triangle.

From this it is visible that only triangles t_{12}, t_{23} and t_{32} are retained which are renamed as t_{b1}, t_{b2} and t_{b3} as shown in Fig.15. For this new region, the set of boundary edges is now given by: E= [e_1 e_2 e_3 e_4 e_5 e_6]. The set of incident triangles on each boundary edge is extracted from the set of triangles DT described in section 3 of data structure. As shown in Fig.15, for one of the edges e_2 it is given by: T_i=[t_{i1} t_{i2} t_{i3} t_{i4}]. Further, set of boundary triangles is extracted from the growing region and is given as: T_b=[t_{b1} t_{b2} t_{b3}]. Now, the steps explained from above are repeated and this way the growth of the region continues.

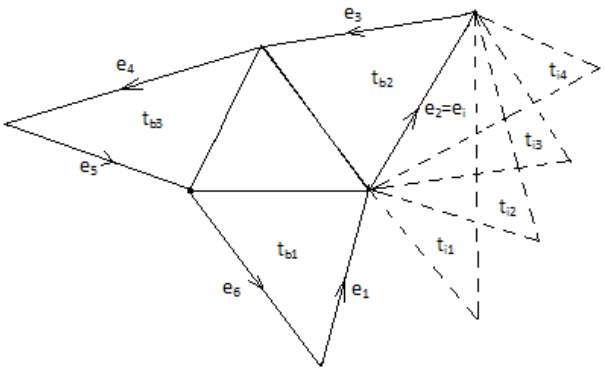


Fig. 15: The New Region after Insertion of Triangles and Triangles Incident on One of the Boundary Edge.

4.3. Topological examination

The topological examination is done for the newly inserted triangles in the growing region S. During region growing process there is a possibility that triangulated surface may result into a non-manifold surface. In fact a manifold surface is one in which each edge shares not more than two triangles. As shown in Fig.16 edge e_1 shares more than two triangles (triangles t_{b1}, t_{i1} and t_{i2}). So, the surface represented by t_{b1}, t_{i1} and t_{i2} is non-manifold surface. Further neck vertices may also be generated. The presence of above two will obstruct the formation of water tight triangulated model. Hence, there is need to examine and eliminate above topological disorders.

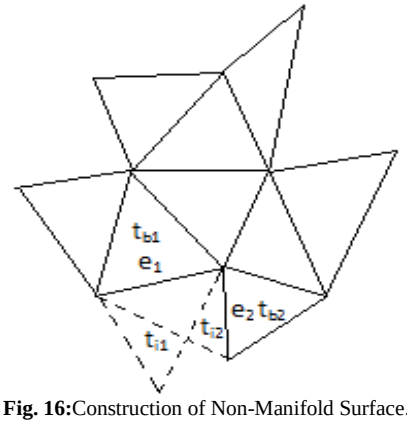


Fig. 16: Construction of Non-Manifold Surface.

4.4. Examination for non-manifolds

It can be explained with the help of Fig.16. In Fig.16, during region growing process edges e_1 and e_2 were found out to be boundary edges. Out of all the triangles on edge e_1 triangle t_{b1} was found to be suitable as it has minimum circum-radius and included angle θ less than $(5\pi/6)$. Similarly out of all the incident triangles on edge e_2 triangle t_{i2} was found to be suitable. However the triangle t_{i2} is also having e_1 as one of the edges. So, as can be seen from Fig.16 on edge e_1 three triangles are falling which satisfies the circum-radius and included angle condition. But this is the case of non-manifold model. To avoid this situation, after adding new triangles to the growing region, a list of triangles on each boundary edge is generated and if any boundary edge shares more than two triangles following procedure is used:

1) The included angles between boundary triangle (e.g. t_{b1} in Fig.16) and triangles added (triangles t_{i1} and t_{i2}) on boundary edge (edge $e_1$in Fig.16) are calculated using the procedure discussed before.
2) The incident triangle which has minimum included angle with the boundary triangle is retained and others are deleted from the new region.

Also to avoid the consideration of the same triangle again and construction of the non manifold it is necessary that the triangles which have been added in the growing region S and the triangles sharing the non-boundary edge must be taken out from the set DT.

4.5. Examination for neck vertices

Fig. 17 illustrates the one ring neighborhood of a vertex v_i in terms of its adjacent vertices(v_1, v_2, v_3, v_4, v_5, v_6), edges(e_1, e_2, e_3, e_4, e_5, e_6) and triangles(t_1, t_2, t_3, t_4, t_5, t_6). For an orientable manifold triangulated model all the vertices must have similar neighborhood. No vertices should be attached with any other triangle except its one ring triangle as shown in Fig.17. However, in region growing process there is possibility of formation of neck vertex. As shown in Fig. 18, a neck vertex is a non-boundary vertex which is connected by a triangle other than the one ring of the triangles. To avoid the formation of neck vertex, at every step of region growing new non-boundary vertices are found out. In Fig.19 vertices c,e and j are non-boundary vertices. It is obvious from Fig.19 that the vertices which are sharing only non-boundary edges are non-boundary vertices. The list of non-boundary vertices can be prepared by first having the list of all the vertices (vertices a,b,c,d,e,f,g,h,i,j and k in Fig.19) which are on the growing region S. Also, the list of vertices which are lying on the boundary edge (vertices a,b,c,d,e,f,g and h in Fig.19) can be found out. Now, the list of non-boundary vertices (vertices i,j and k) can be obtained by deleting the vertices in the second list from the first list.Further, a list of all the triangles incident on these vertices are extracted.This step can be done directly as it was mentioned in section 3 that at the time of prepration of list of triangles, the triangles were prepared in two ways one by their edges and second by their vertices (Fig.7). So, from the list of triangles representing them in terms of their vertices the triangles containing these vertices are extacted and deleted from set DT. This will result into growing region free from neck vertices.

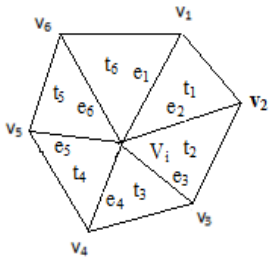


Fig. 17: One Ring Neighborhood of A Vertex V_i.

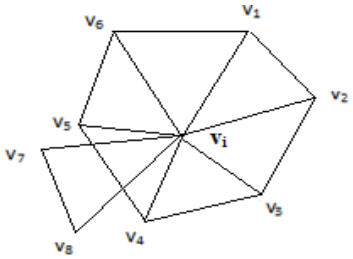


Fig. 18: Formation of Neck Vertex V_i Due to the Joining of Triangle $V_IV_7V_8$.

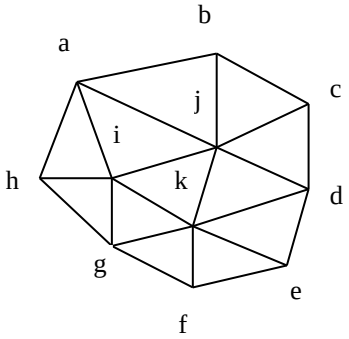


Fig. 19: Vertices A-J in Growing Region S.

4.6. Hole filling

In region growing process there is a possibility of hole formation due to missing data. Fig.20 shows a view of the model with holes. Hence, there is a need to identify the holes and fill them

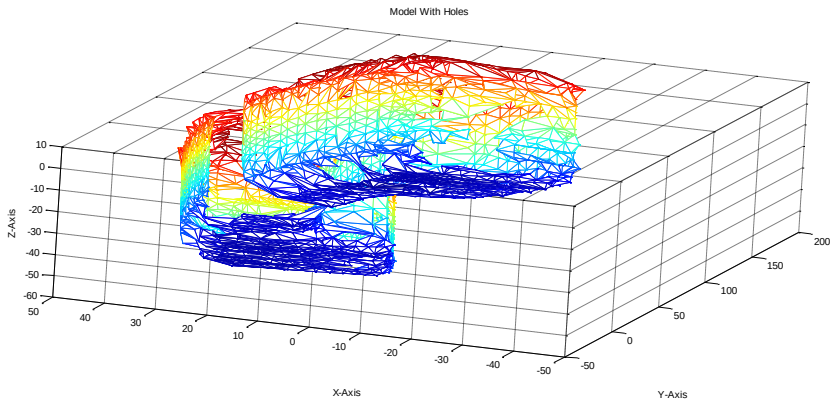


Fig. 20: Holes Present on Model.

In the present work holes have been identified and filled as described below:

1) The boundary vertices of growing region are extracted.

2) The loops made by these boundary vertices are found out. For example in Fig. 21 two loops are present namely v_1,v_2-----v_8 and v_9,v_{10}---v_{21}.
3) If more than one loops are present, it indicates the presence of hole. The largest loop is considered to be boundary of growing region and other smaller loops are considered as holes.
4) The holes are filled by using advancing front mesh generation technique[19]. According to it firstly the angle θ_i between two adjacent boundary edges (e_i and e_{i+1}) at each boundary vertex v_i of a hole is computed as shown in Fig.22. Starting from the vertex v_i with the smallest angle θ_i new triangles are created according to the three rules as shown in Fig.23(a), (b) and (c). Again angle θ_i between two adjacent boundary edges at each boundary vertex incorporating the newly generated vertices is computed and the procedure is repeated till it fills the hole.

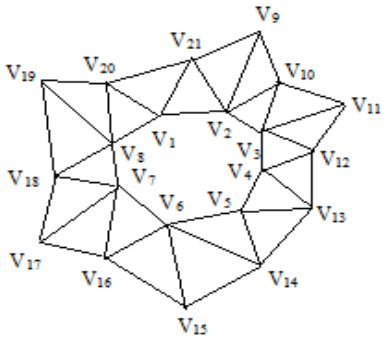


Fig. 21: Two Loops of the Boundary Vertices.

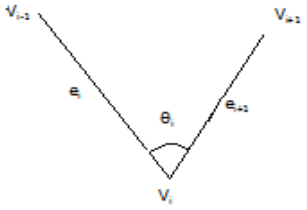


Fig.22: Angle Θ_i between Two Edges E_i and E_{i+1}.

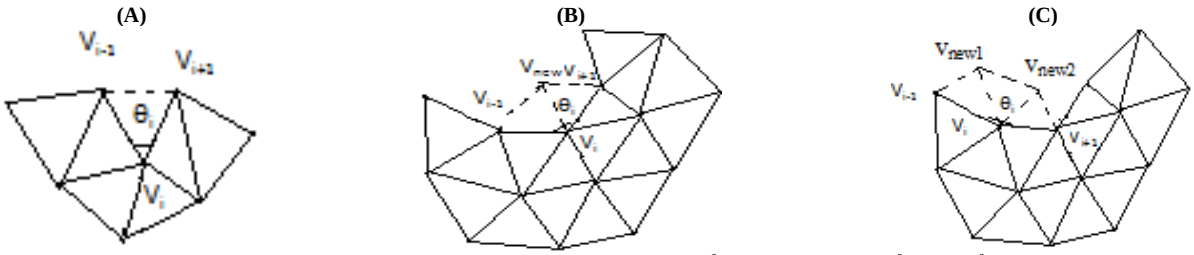


Fig. 23: Creation of New Triangles According to Three Rules (A) Rule-I when $\Theta_i \leq 75^0$ (B) Rule-II when $75^0 < \Theta_i \geq 135^0$ (C)Rule-III When $\Theta_i > 135^0$.

5. Results

As given earlier telephone receiver is chosen as the object for applying the algorithm discussed above. The coordinates of the points covered by fixture could not be measured. No attempt has been made in the present work to fill this gap. The seed triangle as explained in section 4.1 was found on the top face of the model. The triangles were attached on the boundary edges of the growing region according to section 4.2.

Fig.24 shows a view of the generated model before applying topological examination and hole filling processes. In this figure many holes are visible. Further, as the step of topological examination is not incorporated, several neck vertices and non-manifolds were found to be present in triangulated model. Fig.25 (a) shows a non-manifold surface created in triangulated model and Fig.25(b) shows one of neck vertex extracted from triangulated model. Fig.26 shows the same view of the object of Fig.24 after incorporating topological examination and hole filling processes Figs.27(a) and(b) shows the other views of the final model. It can be seen that finally a water tight manifold model is obtained without any topological disorder and holes.

Finally, Fig.28 demonstrates the growing process of triangulated model. It is seen that the triangles are attached only on the surface of the model and the interior of the model is empty without leaving any space on the surface of the model except at the place of fixture.

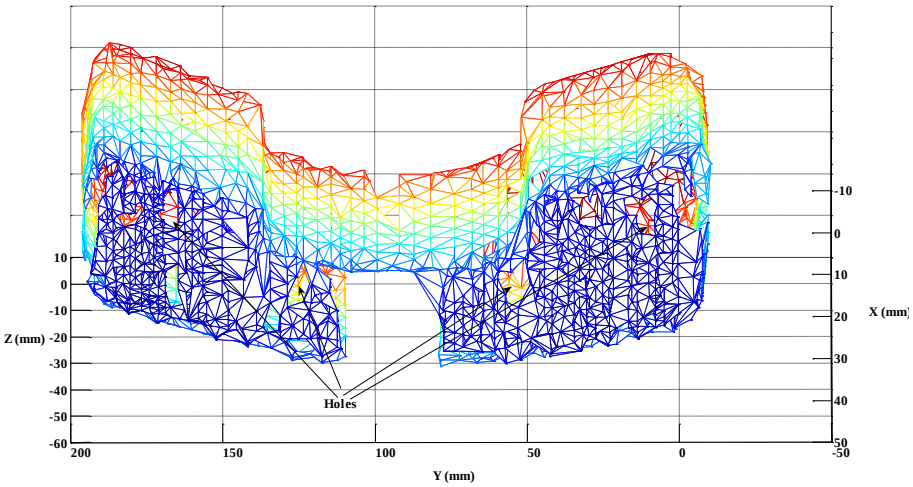


Fig. 24: Triangulated Model Generated Using DBRG Algorithm Not Incorporating Hole Filling Process and Toplogical Examination.

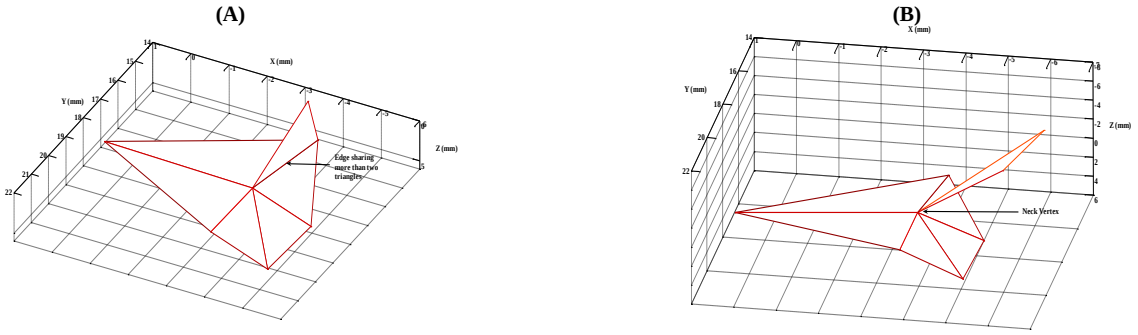


Fig. 25: A) A Non-Manifold Surface Extracted from B) A Neck Vertex Extracted from Triangulated Model Triangulated Model.

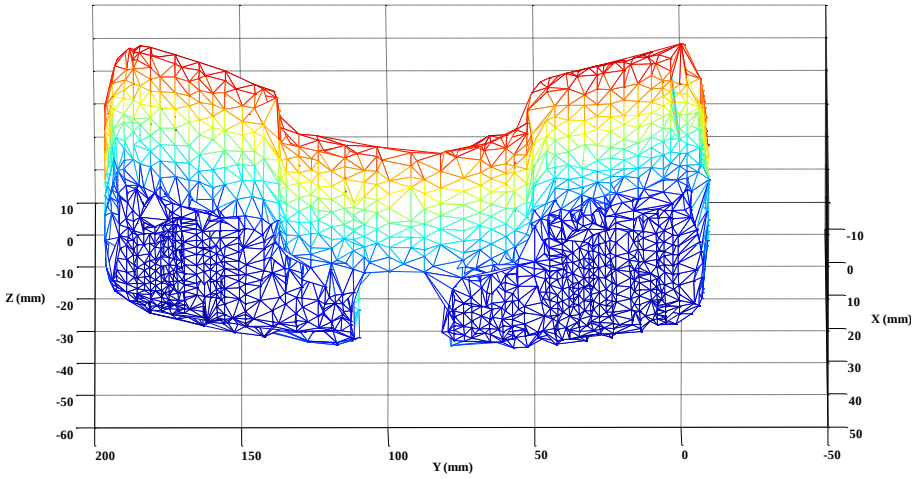


Fig. 26: Triangulated Model Generated Using DBRG Algorithm Incorporating Hole Filling Process and Topological Examination.

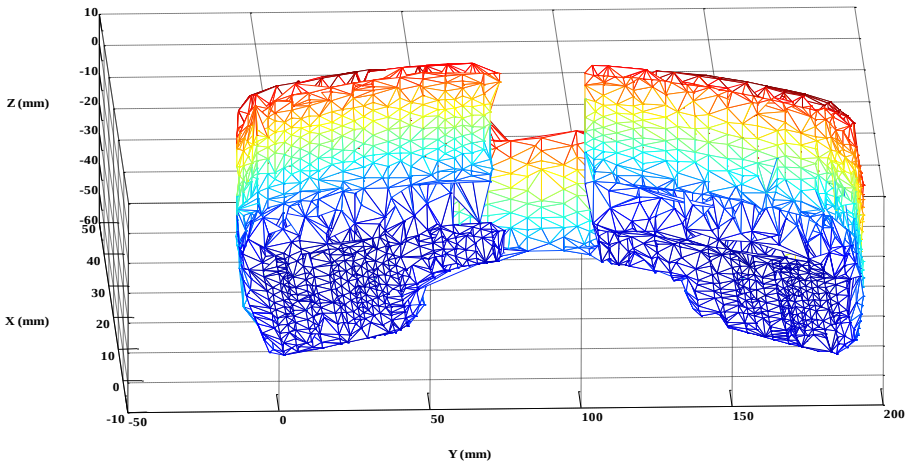


Fig. 27: A) Top and Front Face of the Triangulated Telephone Reciever Model.

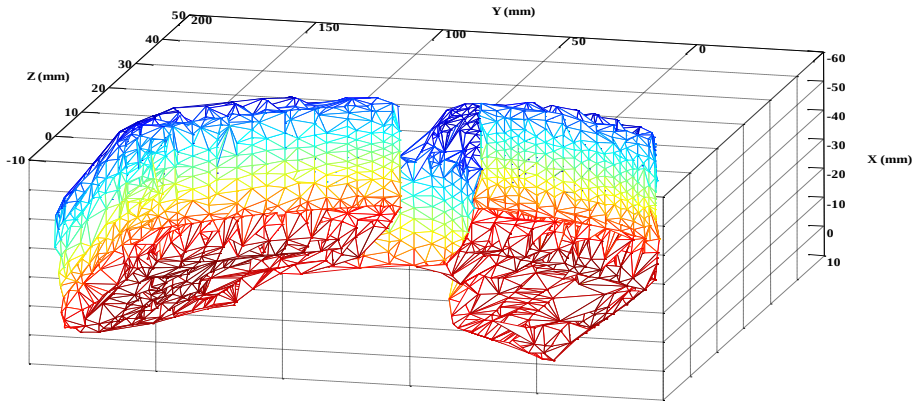


Fig. 27: B) Top, Back and One of the Side Faces of the Triangulated Telephone Reciever Model.

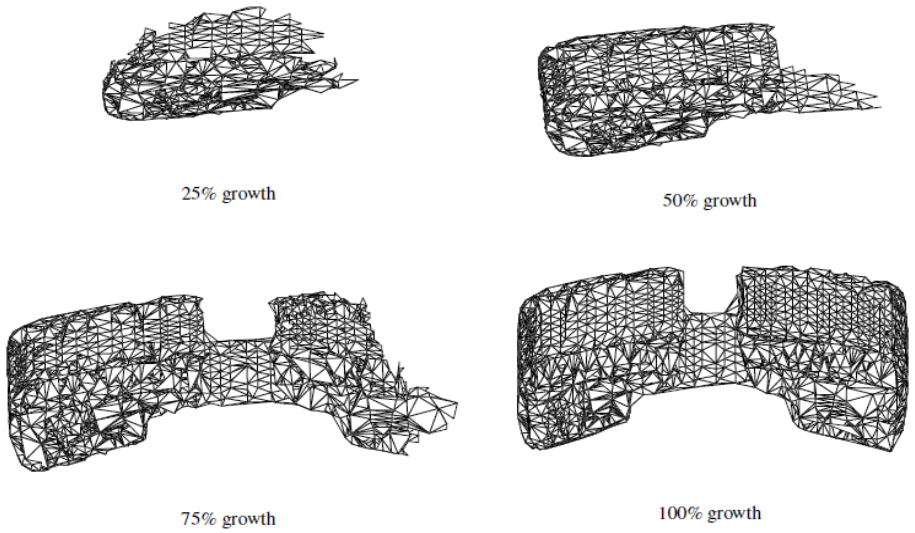


Fig. 28: Demonstration of Growing Process of Telephone Receiver Model.

6. Conclusion

In this work an algorithm is suggested for reconstruction of triangulated model that holds the advantages ofboth delaunay based and region growing approaches. To test the proposed algorithm telephone receiver is chosen as an object. The input of the algorithm is the unorganized points collected on high precision 3D coordinate measuring machine. The output is an orientable manifold triangulated surface. One of the advantages of suggested algorithm is that no post processing is required as hole filling and topological examination is done during the growing process itself. The region growing takes place more smoothly along the faces of the object when algorithm is applied by incorporating hole filling process and topological examination. Further, the holes and topological disorders like neck vertices and non-manifold surface disappeared when algorithm is applied by incorporating hole filling process and topological examination. The triangulated model created so can be used for subsequent processes of reverse engineering like segmentation and surface fitting.

References

[1] M. Vieira, K. Shimada, Surface mesh segmentation and smooth surface extraction through region growing, Computer Aided Geometric Design, 22 (2005) 771-792https://doi.org/10.1016/j.cagd.2005.03.006.

[2] G. Lavoue, F. Dupont, A. Baskurt, A new CAD mesh segmentation method, based on curvature tensor analysis, Computer Aided Design, 37, (2005) 975-987. https://doi.org/10.1016/j.cad.2004.09.001.

[3] M.E. Algorri, F. Schmitt, Surface reconstruction from unstructured 3D data, Computer Graphics forum, 15, 1 (1996) 47-60. https://doi.org/10.1111/1467-8659.1510047.

[4] J. Dan, W. Lancheng, An algorithm of NURBS surface fitting for reverse engineering, International Journal of Advances in Manufacturing Technology 31(2006) 92-97. https://doi.org/10.1007/s00170-005-0161-3.

[5] J.D. Boissonnat, Gometric structures for three dimensional shape representation, ACM Transactions on Graphics,3, 4 (1984) 266-286. https://doi.org/10.1145/357346.357349.

[6] N. Amenta, M. Bern, M. Kamvysselis, A new Voronoi based surface reconstruction algorithm, In: Proceedings of SIGGRAPH, (1998) 415-421.https://doi.org/10.1145/280814.280947.

[7] N. Amenta, S. Choi, R.V. Kolluri, The power crust, Proceedings of sixth ACM symposium on solid modelling and applications, Ann Arbor, MI, USA (2001) 249-266. https://doi.org/10.1145/376957.376986.

[8] E. Menel, H. Muller, Graph based surface reconstruction using structures in scattered point sets, Proceedings of CGI'98 (Computer Graphics International) (1998) 298-311

[9] F. Bernardini, C. Bajaj, F. Chen, D. Schikore, Automatic reconstruction of 3D CAD models from digital scans, International Journal of Computational Geometry and Applications, 9, 4-5 (1999) 327-369 https://doi.org/10.1142/S0218195999000236.

[10] F. Bernardini, J. Mittleman, H. Rushmeier, C. Silva, G. Taubin, The ball pivoting algorithm for surface reconstruction, IEEE Transactions on Visualisation and Computer Graphics, 5, 4 (1999) 349-359. https://doi.org/10.1109/2945.817351.

[11] M. Gopi, S. Krishnan, A fast and efficient projection based approach for surface reconstruction, High Performance Computer Graphics, Multimedia and Visualisation, 1,1(2000) 1-12.

[12] S. Petitjean, E. Boyer, Regular and non-regular point sets: Properties and reconstruction, Computational Geometry, 19, 2-3 (2001),101-126. https://doi.org/10.1016/S0925-7721(01)00016-5.

[13] J. Huang, C.H. Menq, Combinatorial manifold mesh reconstruction and optimization from unorganized points with arbitrary topology, Computer Aided Design, 34, 2 (2002) 149-165.https://doi.org/10.1016/S0010-4485(01)00079-3.

[14] C.S. David, A greedy delaunay based surface reconstruction algorithm, Research Report INRIA , 2002

[15] W. Sun, C. Bradley, Y.F. Zhang, H.T. Loh, Cloud data modelling employing a unified, non-redundant triangular mesh, Computer Aided Design, 33 (2001) 183-193. https://doi.org/10.1016/S0010-4485(00)00088-9.

[16] https://en.wikipedia.org/wiki/Delaunay_triangulation

[17] C.C. Kuo, H.T. Yau, Reconstruction of virtual parts from unorganized scanned data for automated dimensional inspection, Journal of Computing and Information Science in Engineerin, Transactions of the ASME,3, 1 (2003) 76-86. https://doi.org/10.1115/1.1565354.

[18] C. K. Chuan, H.T. Yau, A delaunay based region growing approach to suface reconstruction from unorganized points, Computer Aided Design, 37, (2005) 825-835. https://doi.org/10.1016/j.cad.2004.09.011.

[19] W. Zhao, S. Gao, H. Lin, A robust hole filling algorithm for triangular mesh, The Visual Computer, 23,12 (2007) 987-997. https://doi.org/10.1007/s00371-007-0167-y.